Published in final edited form as:
Synapse. 2013 September ; 67(9): 596–608. doi:10.1002/syn.21665.

Evaluation of Serotonin 5-HT$_{1A}$ Receptors in Rodent Models using [^{18}F]Mefway PET¶

Neil Saigal[1,a], **Alisha K. Bajwa**[1], **Sara S. Faheem**[1], **Robert A. Coleman**[1,b], **Suresh K. Pandey**[1,c], **Cristian C. Constantinescu**[1], **Vanessa Fong**[1], and **Jogeshwar Mukherjee**[1]

[1]Preclinical Imaging, Department of Radiological Sciences, University of California, Irvine, CA, USA

Abstract

Introduction—Serotonin 5-HT$_{1A}$ receptors have been investigated in various CNS disorders, including epilepsy, mood disorders and neurodegeneration. [^{18}F]Mefway (*N*-{2-[4-(2'-methoxyphenyl)piperazinyl]ethyl}-*N*-(2-pyridyl)-*N*-(*cis/trans*-4'-[^{18}F]fluoromethylcyclohexane)-carboxamide) has been developed as a suitable positron emission tomography (PET) imaging agent for these receptors. We have now evaluated the suitability of [^{18}F]*trans*-mefway in rat and mouse models using PET and computerized tomography (CT) imaging and corroborated with *ex vivo* and *in vitro* autoradiographic studies.

Methods—Normal Sprague-Dawley rats and Balb/C mice were used for PET/CT imaging using intravenously injected [^{18}F]*trans*-mefway. Brain PET data were coregistered with rat and mouse magnetic resonance (MR) imaging template and regional distribution of radioactivity was quantitated. Select animals were used for *ex vivo* autoradiographic studies in order to confirm regional brain distribution and quantitative measures of binding, using brain region to cerebellum ratios. Binding affinity of *trans*-mefway and WAY-100635 was measured in rat brain homogenates. Distribution of [^{18}F]*trans*-4-fluoromethylcyclohexane carboxylate ([^{18}F]FMCHA), a major metabolite of [^{18}F] *trans*-mefway, was assessed in the rat by PET/CT.

Results—The inhibition constant, K_i for *trans*-mefway was 0.84 nM and that for WAY-100635 was 1.07 nM. Rapid brain uptake of [^{18}F]*trans*-mefway was observed in all rat brain regions and clearance from cerebellum was fast and was used as a reference region in all studies. Distribution of [^{18}F]*trans*-mefway in various brain regions was consistent in PET and *in vitro* studies. The dorsal raphe was visualized and quantified in the rat PET but identification in the mouse was difficult. The rank order of binding to the various brain regions was hippocampus>frontal cortex>anterior cingulate cortex>lateral septal nuclei>dorsal raphe nuclei.

Conclusion—[^{18}F]*trans*-Mefway appears to be an effective 5-HT$_{1A}$ receptor imaging agent in rodents for studies of various disease models.

Keywords

Mefway; MicroPET; Serotonin; 5-HT$_{1A}$ receptors; WAY-100635

¶Dedicated to the memory of Neil Saigal

Address Correspondence to: Jogesh Mukherjee, Ph.D. Preclinical Imaging Medical Sciences B 140 Department of Radiological Sciences University of California-Irvine Irvine, CA 92696-5000 Tel# (949) 824-2018 FAX # (949) 824-2344 j.mukherjee@uci.edu.
[a]Deceased September 8, 2011
[b]Present address: Department of Cognitive Science, University of California, Irvine
[c]Present address: Lantheus Medical Imaging, Boston, MA

1. INTRODUCTION

Serotonin 5-HT_{1A} receptors have been investigated in a number of CNS disorders, including depression, anxiety, epilepsy, Parkinson's disease (PD) and Alzheimer's disease (AD) (Borg, 2008; Mehrotra et al., 2008; Parsey, 2010; Paterson et al., 2013). Two areas of potential clinical applications of serotonin 5-HT_{1A} receptor agents include major depression and epilepsy (reviewed in Parsey 2010). Imaging the serotonin neurotransmitter system in mood disorders, such as depression, electroconvulsive therapy, sleep disorders, mania, bipolar disorder and anxiety have been an area of major focus (for eg., Kennedy and Zubieta, 2004; Lanzenberger et al., 2013; Savitz et al., 2009; Akimova et al., 2009). Relevance of 5-HT_{1A} receptor imaging in epilepsy for surgical planning has been incrementally established (e.g., Assem-Hilger et al., 2010). Only a limited number of serotonin 5-HT_{1A} receptor imaging studies currently exist for AD. A number of animal model studies have strongly suggested that serotonin 5-HT_{1A} receptors have a role in learning and memory (Bert et al., 2008; King et al., 2008). Results in humans are mixed and it has been suggested that the findings may be a result of age range, gender differences, methodological issues, partial volume correction, and potential differences in the cognitive status of the subjects (Borg 2008; Costes et al., 2005; Kepe et al., 2006; Truchot et al., 2008).

It has been suggested that advances in positron emission tomography (PET) imaging to clinical practice require many steps. These include a well-characterized PET radiotracer which is: (1) easily available; (2) is easily quantifiable; (3). is lacking in toxicity; (4) has suitable dosimetry; (5) is available for large multi-center trials, and (6) is amenable to standardization and automation of image analysis (Coenen et al., 2010; Parsey, 2010). [^{18}F]Mefway (Saigal et al., 2006) has been developed to overcome the short half-life, difficult radiosyntheses of [^{11}C]WAY-100635, *in vivo* stability of [^{18}F]FCWAY and low specific binding of [^{18}F]MPPF that are currently being used in human PET studies. Nonhuman primate studies with [^{18}F]mefway indicate promising *in vivo* PET imaging properties which are comparable to [^{11}C]WAY-100635 (Wooten et al., 2011b).

A number of rodent disease models (mice and rats) are currently available and PET imaging studies of the serotonin 5-HT_{1A} receptor on these models will be very useful. Initial nonhuman primate PET imaging studies were carried out using mixture of [^{18}F]*cis*- and *trans*-mefway (Saigal et al., 2006). A comparative study of pure [^{18}F]*cis*-mefway and pure [^{18}F]*trans*-mefway confirmed that the *trans*-isomer provided higher binding potentials in receptor- rich regions (Fig-1; Wooten et al., 2011). Given the small size of the rodent brain, the use of [^{18}F]*trans*-mefway may be more suitable.

Here we report evaluation of [^{18}F]*trans*-mefway (heretofore referred as [^{18}F]mefway) in PET/computerized tomography (CT) studies of rat and mouse brains. *In* vivo rat studies were compared to *ex vivo* rat PET and *ex vivo* autoradiographic brain slices in order to evaluate accuracy of *in vivo* measurements for smaller brain regions, such as the dorsal raphe which innervate the rat forebrain. Sensitivity of [^{18}F]mefway binding to cortical layers of the rat brain was measured in order to assess the *in vivo* utility of [^{18}F]mefway in distinguishing cortical binding. Brain distribution of [^{18}F]mefway was evaluated in mouse PET/CT studies. Brain uptake of the ^{18}F-mefway metabolite, [^{18}F]*trans*-4-fluoromethylcyclohexane carboxylic acid ([^{18}F]FMCHA) was evaluated to assess brain penetration of the metabolite.

2. MATERIALS AND METHODS

2.1 General methods

All chemicals and solvents were of analytical or HPLC grade from Sigma-Aldrich, St. Louis, MO and Fisher Scientific, Hanover Park, IL. [^{3}H]WAY-100635 was purchased from Perkin-Elmer (specific activity 60-86 Ci/mmol). Chromatographic separations were carried out on preparative TLC (silica gel GF 20×20 cm 2000 micron thick; Alltech Assoc. Inc., Deerfield, IL) or silica gel flash column or semi-preparative reverse-phase columns using the Gilson high performance liquid chromatography (HPLC) systems. High specific activity [^{18}F]fluoride ion was produced in the MC-17 cyclotron using oxygen-18 enriched water ([^{18}O] to [^{18}F] using p, n reaction). The >95% pure precursor *trans*-mefway tosylate (*trans*-*N*-{2-[4-(2'-methoxyphenyl)piperazinyl]ethyl}-*N*-(2-pyridyl)-*N*-(4'-toluenesulfonyloxymethylcyclohexane)carboxamide) was prepared in house using modifications of our reported methods (Saigal et al., 2006). The high specific activity [^{18}F]fluoride ion was used in subsequent reactions which were carried out in automated chemistry processing control unit (CPCU). [^{18}F]Fluoride ion radioactivity was counted in a Capintec CRC-15R dose calibrator while low level counting was carried out in a Capintec Caprac-R well-counter. Radioactive thin layer chromatographs were obtained by scanning in a Bioscan system 200 imaging scanner (Bioscan, Inc., Washington, DC). Rat brain slices were prepared at 10-40 μm thickness using a Leica 1850 cryotome. [^{18}F]Fluorine autoradiographic studies were carried out by exposing tissue samples on storage phosphor screens multisensitive, medium MS (Perkin Elmer, Waltham, MA). The apposed phosphor screens were read and analyzed by OptiQuant acquisition and analysis program of the Cyclone Storage Phosphor System (Packard Instruments Co., Boston, MA). A preclinical Inveon dedicated PET scanner (Siemens Medical Solutions, Knoxville, TN) with a transaxial full width at half maximum (FWHM) of 1.46 mm, and axial FWHM of 1.15 mm (Constantinescu and Mukherjee, 2009) was used for the PET studies. Both *in vivo* and *ex vivo* PET images of rat brains were obtained and analyzed using ASIPro VM (Concorde Microsystems Inc., Knoxville, TN) and Pixelwise Modeling Software (PMOD 3.0; PMOD Technologies Ltd, Zurich, Switzerland) software. All animal studies were approved by the Institutional Animal Care and Use Committee of University of California, Irvine.

2.2 Homogenate binding assay

Rat brain homogenate assays using [^{3}H]WAY-100635 were carried out to measure the binding affinity of *trans*-mefway to 5-HT$_{1A}$ receptor. The cerebrum (0.85 g of tissue per assay) of each male rat was isolated and homogenized in 30 mL of assay buffer for 30s (50 mM Tris-HCl, pH 7.6) using Tekmar tissumizer (15s, half maxima speed). The homogenate was centrifuged at 27,000g for 20 min at 4 °C and the supernatant was discarded. The resulting pellet was resuspended in 30 mL of buffer, homogenized, and then centrifuged at 27,000g for 20 min at 4 °C. Once again the supernatant was removed and the pellet was diluted with incubation buffer. A fixed concentration of [^{3}H]WAY-100635 (1 nM) was incubated with the rat homogenate in the presence of various concentrations of *trans*-mefway (10^{-12} to 10^{-4} M) in the assay buffer (50 mM Tris-HCl, pH 7.6). Nonspecific binding was determined by including 10 μM of WAY-100635. Total assay volume was 0.5 mL. To start, 0.2 mL of the rat brain homogenate was added to each test tube containing [^{3}H]WAY-100635, different concentrations of *trans*-mefway and 10 μM of WAY-100635 for nonspecific binding. The assay was done in duplicate and all test tube samples were incubated for 1h in a 37 °C water bath. After incubation a rapid vacuum filtration was implemented through Whatman GF/C filter paper (pre-soaked in 0.1% polyethylamine in 10 mL of millipore water) using Brandel tissue harvester. The filter was washed three times with 5 mL of cold buffer, was transferred to vials with 5 ml Bio-Safe II scintillation cocktail and counted for 10 min in a scintillation counter. The same procedures were followed when

performing the binding assay for WAY-100635 as the test compound. Data was analyzed using the following procedures: (a) the non-specific binding of [^{3}H]WAY-100635 was subtracted for all samples; (b) the specific binding was normalized to 100% (no competitive ligand) and (c) the binding isotherms were fit to the Hill equation (KELL BioSoft software (v 6), Cambridge, U.K.). The dissociation constant, K_d for the [^{3}H]WAY-100635 to serotonin 5-HT_{1A} receptor of 0.59 nM was used (Khawaja et al., 1995).

2.3 Mefway radiolabeling

The radiosynthesis of [^{18}F]*trans*-mefway was performed in an automated CPCU using previously described procedures (Saigal et al., 2006). Briefly, [^{18}F]fluoride ion in $H_2{}^{18}O$ was passed through a QMA-light Sep-Pak (Waters Corp.), pre- conditioned with 3 mL of K_2CO_3, 140 mg/mL, followed by 3 mL of anhydrous acetonitrile. The [^{18}F]fluoride ion trapped in the QMA-light Sep-Pak was then eluted with 1 mL Kryptofix 2.2.2./ K_2CO_3 (360 mg/75 mg in 1 mL of water and 24 mL of acetonitrile) and transferred to the CPCU reaction vessel. The product was purified in a reverse-phase HPLC C18 Econosil column (250×10 mm; Alltech Assoc. Inc.) with 60% acetonitrile:40% water containing 0.1% triethylamine with a flow rate of 2.5 mL/min. The retention time of [^{18}F]mefway was found to be 11 min. The [^{18}F]mefway fraction was collected into a flask and the solvent was removed in vacuo using a rotary evaporator to dryness. The final formulation of [^{18}F]mefway was carried out using approx. 2 to 5 mL of saline (0.9% NaCl INJ) followed by filtration through a membrane filter (0.22 μm) into a sterile dose vial for use in the PET studies. Radiochemical purity was >98% and chemical purity was found to >95% of this formulated product with a specific activity of approximately 74 GBq/μmol at the end of radiosynthesis.

2.4 *In vitro* autoradiography

Sprague-Dawley rats (250-300g) and Balb/C mice (25-30g) were anesthetized and decapitated; the brain was rapidly removed and frozen in isopentane at −20 °C. Horizontal slices were cut 10 μm thick using a Leica 1850 cryotome. Slices contained regions known to have 5-HT_{1A} receptors which include the hippocampus, frontal cortex and dorsal raphe. Brain slices were preincubated in 50 mM Tris-HCl buffer (pH 7.4) for 10 min The slices were then incubated with 1-2 μCi/mL of [^{18}F]mefway at 37 °C for 1h. Nonspecific binding was measured in the presence of 10 μM of WAY-100635. After incubation, slides were washed twice (each wash lasting one minute) with ice-cold buffer. Slides were then quickly dipped in cold deionized water, air dried, and exposed to a phosphor screen for 24h. The autoradiographs were generated using the Phosphor Cyclone Imager. The amount of binding was evaluated in digital light units (DLU/mm^2) using OptiQuant acquisition and analysis program (Packard Instruments Co.).

2.5 *In vivo* rat PET/CT

Male Sprague-Dawley rats (240-310 g) were fasted 24h prior to the time of scan. On the day of the study rats were anesthetized with 4% isoflurane. The subjects were placed on the scanner bed on a warm water circulating heating pad set at 35 °C and kept anesthetized with 2.5% isoflurane delivered via a nose cone. An initial 10-min transmission scan was acquired with a ^{57}Co point source embedded in the scanner. A dose of 24.6 ± 11.3 MBq (specific activity 65 GBq/μmol) [^{18}F]mefway in 0.9% NaCl was prepared in a 1ml syringe with a 25 gauge needle. This dose was injected intravenously into the tail vein of the rat. The animals were scanned in full list mode for 1 to 2h with the head positioned in the center of the field-of-view. List-mode data from the 120 min acquisition were histogrammed in 27 time frames (4 × 30 s, 8 × 1 min, 5 × 2 min, 4 × 5 min, 4 × 10 min, 2 × 20 min). Random events were subtracted prior to reconstruction. All images were reconstructed using Fourier rebinning and 2-dimensional ordered subset expectation maximization (OSEM2D) method (16 subsets, 4 iterations) with an image matrix of 128×128×159, resulting in a pixel size of 0.77

mm and a slice thickness of 0.796 mm. All dynamic images were corrected for radioactive decay. An image calibration was conducted to becquerel per cubic centimeter (Bq/cm^3). using a Ge-68 cylindrical with known activity.

2.6 *Ex vivo* rat brain PET

The rats were sacrificed and the brain was extracted for *ex vivo* microPET imaging after completion of the *in vivo* microPET scans, to ascertain the brain uptake of [^{18}F]mefway . The whole brain was placed in a hexagonal polystyrene weighing boat (top edge side length, 4.5 cm; bottom edge side length, 3 cm) and covered with powdered dry ice. This boat was placed securely on the scanner bed, and a transmission scan was acquired. Subsequently, a 60 minute emission scan was acquired. The reconstruction of the images was similar to the procedure described previously. The images were analyzed using the ASIPro VM and PMOD software.

2.7 *Ex vivo* rat brain autoradiographs

After the *ex vivo* PET acquisition (described in the section "*Ex vivo* rat brain PET") the brain was removed from the dry ice and was rapidly prepared for sectioning. Horizontal sections (40-μm thick) containing brain regions of the hippocampus, lateral septum, frontal cortex, dorsal raphe and cerebellum were cut using the Leica CM1850 cryotome. The sections were air-dried and exposed to phosphor films overnight. The films were read using the Cyclone Phosphor Imaging System. Regions of the same size were drawn and analyzed using the OptiQuant software. The activity of [^{18}F]mefway was measured in DLU/mm^2. Binding of [^{18}F]mefway was quantified as ratios between activity in the target region to that in the cerebellum.

2.8 *In vivo* mouse PET/CT

Balb/C mice were used for the *in vivo* [^{18}F]mefway PET experiments. Mouse PET/CT studies with [^{18}F]mefway were carried out as previously described (Constantinescu et al., 2012). The Inveon PET and MM CT scanners were placed in the "docked mode" for combined PET/CT experiments. All images were calibrated in units of Bq/cm^3 by scanning a 55 mL [^{18}F]fluoride ion solution with known activity and reconstructing the acquired image with parameters identical to those of rat [^{18}F]mefway images. The average injected dose of [^{18}F]mefway was 9.5 ± 2.9 MBq (specific activity 65 GBq/μmol) for mouse. PET data acquisition was followed by a CT scan for attenuation correction and anatomical delineation of PET images. The PET images were spatially transformed to match the reconstructed CT images. PET images were corrected for random coincidences, attenuation and scatter. The CT projections were acquired with the detector-source assembly rotating over 360 degrees and 720 rotation steps. A projection bin factor of 4 was used in order to increase the signal to noise ratio in the images. The CT images were reconstructed using cone-beam reconstruction with a Shepp filter with cutoff at Nyquist frequency and a binning factor of 2 resulting in an image matrix of 480 × 480 × 632 and a voxel size of 0.206 mm.

2.9 Image analysis

Processing of reconstructed images was performed with PMOD software package. PET rat images were normalized to the standard space described by the stereotaxic coordinates (Paxinos and Watson, 1986) via co-registration to an MRI rat template (Schweinhardt et al., 2003). The size of the template image was 80 × 63 × 108 voxels with a voxel size of 2 mm, with bregma as the origin of coordinates system. The dynamic PET images between 20 and 60 min were first summed, and the summed image was resliced using the fusion toolbox of PMOD to match the size of the magnetic resonance (MR) template. The summed image was then manually co-registered to the MR brain template and therefore normalized to the

Paxinos and Watson brain atlas. The resulting transformation matrix for each subject was subsequently applied to all the images in the dynamic series. 3D volumes of interest (VOIs) were drawn on the MR template for the hippocampus, lateral septal nuclei, anterior cingulate cortex, frontal cortex, dorsal raphe nucleus, and cerebellum. The placing of the VOIs was guided by examination of the Paxinos and Watson rat atlas. All VOIs were copied to the PET images and time activity curves (TACs) were extracted for each VOI from the dynamic PET data.

Kinetic analysis of rat *in vivo* PET studies was performed using kinetic analysis toolbox in PMOD. Distribution volume ratio (DVR) in each selected brain region was calculated for using Logan non-invasive method (LNI) (Logan et al., 1996). Binding potential (BP_{ND}) was calculated as "DVR-1." Cerebellum was used as a reference region since it is known not to be enriched with serotonin 5-HT_{1A} receptors. LNI method requires prior estimation of the blood-tissue tracer transfer rate in the cerebellum, k_2', which was computed indirectly from fitting the simplified reference tissue model (SRTM) (Lammertsma and Hume, 1996) to the hippocampus curve using a Marquandt optimization algorithm with 200 iterations. The estimated k_2' for each subject was then fixed and used subsequently for Logan analysis of all other brain regions. The cutoff of Logan plot was determined based on a preset error of 10% between the fit and the data.

Mouse *in vivo* PET images, summed over 20-60 min interval, were co-registered to a MRI mouse brain template (Ma et al., 2005) of size 192 × 96 × 256 voxels with a voxel size of 2 mm, which was preliminarily scaled by a factor of 20. VOIs representing hippocampus, lateral septal nucleus, frontal cortex and cerebellum were manually drawn on the MR template and copied to PET images. The BP_{ND} were computed using the interval method (Ito et al., 2011) based on the tissue ratios with respect to cerebellum over 60-90 min of the scan.

3. RESULTS

3.1 *In vitro* binding

In vitro binding affinity of *trans*-mefway (Fig-1) in rat brain homogenates using [^{3}H]WAY-100635 yielded an IC_{50} of 3.11 nM compared to 3.97 nM for WAY-100635. These IC_{50} values are consistent with our previously reported values for mefway (IC_{50} of 3.11 nmol/L), which was similar to the affinity of WAY-100535 (IC_{50} of 3.97 nmol/L) using rat brain slices labeled with [^{18}F]mefway (Saigal et al., 2006). Inhibition constants were calculated using the Cheng-Prusoff equation ($Ki=IC_{50}/(1+(\text{conc of } [^3H]WAY)/K_d)$; Cheng and Prusoff, 1973) and a K_d= 0.37 nM for [^{3}H]WAY-100635 (Khawaja et al., 1995). The inhibition constant, K_i for *trans*-mefway was 0.84 nM and that for WAY-100635 was 1.07 nM. This is in agreement with previously reported K_i values for WAY-100635 (Khawaja et al., 1995).

3.2 ^{18}F-Mefway rat PET/CT studies

Rat brain distribution of [^{18}F]radioactivity after [^{18}F]mefway injection as measured by dynamic PET is shown in Fig-3. Two levels of the rat brain orthogonal slices are shown and include the MR template (A), PET/MR coregistered (B), the CT slice (C) acquired on the same animal and the coregistered PET/CT slices (D). The top set (rows 1-3) is showing the dorsal hippocampus (cross-hair on the hippocampus in the CT), showing binding of [^{18}F]mefway to the hippocampus, enthorinal cortex, lateral septal nucleus, anterior cingulate cortex, frontal cortex and cerebellum. The cerebellum had the least amount of [^{18}F]mefway binding. Using the CT areas of distinct extracranial uptake were identified (marked with an asterisk in the coregistered PET/CT image). The orthogonal slices shown in rows 4-6 were

obtained from the ventral brain regions and the cross-hair cursor is positioned on the dorsal raphe region in the MR template (A) to which the PET is coregistered to. Binding of [^{18}F]mefway is evident in the 3 planes and also visualized in the hippocampus. Extracranial activity as identified using the PET/CT coregistered images may influence some of the cortical regions of interest. Cerebellum was used as the reference region and appears not to be affected from extracranial spillover.

A typical TAC of intravenously injected [^{18}F]mefway in the rat is shown in Fig-4A. Rapid brain uptake of [^{18}F]mefway was observed in all brain regions. Faster clearance from cerebellum was observed and this was used as a reference region in all studies. Significant amount of [^{18}F]mefway binding remained in the receptor-rich regions approx. 60 min after injection. The rank order of [^{18}F]mefway binding to the various brain regions 60 min after injection was hippocampus>frontal cortex>anterior cingulate cortex>lateral septal nucleus>dorsal raphe nucleus (Fig-4B). Ratio of brain regions versus cerebellum ranged from approx. 9 for hippocampus to 3 for dorsal raphe nucleus.

3.3 *Ex vivo* rat MicroPET and rat autoradiography

After the *in vivo* scans of [^{18}F]mefway, selected rats were chosen to carry out an *ex vivo* MicroPET scan. Ex vivo imaging of the brain was carried out for another 60 min. Results in Fig-5A-C clearly show binding of [^{18}F]mefway in the hippocampus, frontal cortex, septal nuclei and dorsal raphe. Very little binding was observed in the cerebellum. This remained consistent in the *in vivo* image (A), *ex vivo* image (B) and *ex vivo* autoradiography (C). A correlation of *in vivo* binding versus *ex vivo* autoradiography is shown in Fig-5D with R^2=0.93 when frontal cortex and dorsal raphe nucleus were excluded. The small size (<1mm^3) of the dorsal raphe (Bellido et al., 2002) in the rat brain effects accurate quantitation *in vivo* due to from partial volume effects. Ratios of brain regions versus cerebellum measured in *ex vivo* autoradiographic binding of [^{18}F]mefway was correlated with reported binding of a 5-HT$_{1A}$ receptor agonist, [^{3}H]8-hydroxy-2-(di-n-propylamino)tetralin ([^{3}H]8-OH-DPAT).binding in the rat brain (Duncan et al., 1998).

Detailed analyses of *ex vivo* autoradiographs are shown in Fig-6A-D. Significant binding in 3 layers of the frontal cortex is shown in Fig-6A with the middle cortical layer and the inner cortical layer showing higher levels of binding. Binding in the anterior cingulate cortex was higher than frontal cortical layers as seen in Fig-6B, while enthorinal cortex exhibited the highest cortical binding (outer enthorinal cortex greater than inner). High binding areas included the hippocampal regions, CA1, CA2, CA3 and dentate gyrus as well as lateral septal nuclei. Ratios of the five high binding regions with respect to the cerebellum exceeded 20 (Fig-6E), while ratios of the cortical regions ranged from 3 to 18 (Fig-6F).

3.4 ^{18}F-Mefway mouse PET/CT studies

Mouse brain distribution of [^{18}F]mefway was similar to that measured for the rat *in vitro* binding. Fig-7A shows significant binding in the hippocampus, dorsal raphe nucleus, lateral septal nucleus and the cortical regions such as anterior cingulate cortex and enthorinal cortex. Ratios of binding with respect to cerebellum exceeded 20 for hippocampus and dorsal raphe nucleus while for the cortical areas and lateral septal nucleus ratios ranged from 10 to 18 (Fig-7B). Brain localization of [^{18}F]mefway in the mouse was rapid in receptor-rich regions and cerebellum showed little retention. This is consistent with the observations in the rat brain. Regions with high binding included the hippocampus, lateral septal nucleus and cortical regions. This binding was confirmed by MR/PET coregistration (Fig-7C). Time-activity curves of [^{18}F]mefway in these regions showed significant retention over the course of the PET scan.

3.5 ^{18}F-metabolite study

In order to evaluate the ability of the [^{18}F]mefway metabolite, [^{18}F]FMCHA (Fig-8), to traverse the blood brain barrier and have any significant amount of retention in the brain, we prepared [^{18}F]FMCHA (Liang et al., manuscript in preparation) and tested it in the rat model.

Localization of [^{18}F]FMCHA was extensive in peripheral regions such as the liver, with little uptake in the brain as seen in the images in Fig-8B,C. Even at later times, there was not a significant amount of defluorination of this metabolite since bone uptake remained low.

4. DISCUSSION

Binding affinity of *trans*-mefway *in vitro* in the rat brain correlated closely with the *in vivo* affinity measured for [^{18}F]mefway in the monkeys using PET (K_i= 0.84 nM for rats *in vitro*, and *in vivo* equilibrium dissociation constant, K_{Dapp}= 4.3 nM for monkeys in vivo; Wooten et al., 2012). Our previously reported studies of WAY-100635 and mefway in rat brain slices found very similar binding affinity for the two compounds (Saigal et al., 2006). This similarity of binding affinity between WAY-100635 and mefway and their similar backbone chemical structure resulted in the very similar *in vivo* imaging characteristics reported in the monkeys (Wooten et al., 2011). It must be noted that WAY-100635 has been shown to be an antagonist at the 5-HT_{1A} receptor (Khawaja 1995), while the intrinsic antagonistic activity of mefway has yet to be determined.

Our goal here was to delineate the brain binding characteristics of [^{18}F]mefway in vivo in rodents using PET. Mefway was able to bind to 5-HT_{1A} receptors *in vivo* in the rodents measureable by PET. This was confirmed both in the rats and mice. Using PET/CT and coregistered PET and MR images of the rat brain, localization of [^{18}F]mefway was confirmed in 5-HT_{1A} receptor-rich brain regions such as the hippocampus, dorsal raphe nucleus, anterior cingulate cortex, lateral septal nucleus, enthorinal cortex and other areas. In the rats the accuracy of the *in vivo* measurements was assessed using *ex vivo* PET imaging and autoradiography of the brain slices of the *ex vivo* brain. Excellent binding was measured in the ex vivo autoradiographs and therefore served as the ‘gold standard’ for [^{18}F]mefway binding in the various brain regions. Correlation of the findings of *in vivo* PET with autoradiographs showed good consistency in all of the regions except for the frontal cortex (which may be affected by spillover of extracranial activity) and dorsal raphe (which may be affected by partial volume effect due to its small size) as described in Fig-5D. Additionally, [^{18}F]mefway binding in *ex vivo* autoradiographs correlated well with reported measures of [^{3}H]WAY-100635 and [^{3}H]8-OH-DPAT concentrations in the rat brain (Khawaja, 1995; Duncan et al., 1998).

The mouse brain shows similar results to that of the rat. [^{18}F]Mefway was able to selectively localize in the receptor-rich regions that were found using *in vitro* measures. Hippocampus, lateral septal nucleus and frontal cortex were more easily discernible *in vivo* than *in vitro*, where several other areas such as the dorsal raphe nucleus and enthorinal cortex also showed prominent [^{18}F]mefway binding. MR-PET template assisted in the delineation of the different mice brain regions. The small size of the mice brain affects the accurate measurement of small regions such as the dorsal raphe nucleus. Binding kinetics measured in mice varied from those seen in the rats and may be indicative of a species difference and the possible role of the efflux transporter (observed with other 5-HT_{1A} radioligands, Paterson et al., 2013) cannot be ruled out.

The ability of [^{18}F]mefway to localize in the dorsal raphe was assessed *in vivo*. Both the *ex vivo* microPET and *ex vivo* autoradiographs clearly showed the presence of [^{18}F]mefway

binding in the dorsal raphe. Only one recent report on 5-HT_{1A} receptors has evaluated the dorsal raphe in the rodent model (Saijo et al., 2012) but has been characterized in nonhuman primates (Wooten et al., 2011b) and in humans (Parsey et al., 2000). Since this region is where the serotonergic pathways emerge, the ability of [^{18}F]mefway to measure this region *in vivo* in the rodent model using [^{18}F]mefway is highly significant. It will allow for studies on the role of the dorsal raphe in various disease rodent models including antidepressant drug effects using small animal PET imaging studies.

Differential distribution of serotonin 5-HT_{1A} receptors in the cortical layers have been reported in postmortem human brain autoradiographic studies (Duncan et al., 1998). We have previously shown differential cortical layer binding in the dog brain using [^{18}F]mefway autoradiography (Dinh et al., 2009). Analysis of the cortical layers in the rat brain revealed higher binding in the middle and inner layers of the frontal cortex (Fig-6A). The layers were visible in the *ex vivo* autoradiographs, however, separation of the layers *in vivo* PET was not attainable and therefore shows the cortex as a single layer.

Metabolism of the derivatives of WAY-100635 used for PET imaging has been a significant concern (Pike 2009). Cleavage of the amide bond in these derivatives (Fig-8A) decreases plasma concentration of the parent molecule, consequentially giving rise to the radiolabeled cyclohexanecarboxylate metabolite. This then raises the potential possibility of the radiolabeled metabolite traversing back into the brain. Additionally, in the case of some of the [^{18}F]fluorine labeled agents, cleavage of the radioactive fluorine also occurs which makes it difficult to accurately quantify outer cortical areas due to spillover of [^{18}F]fluoride ion activity from the skull (Carson et al., 2003). However, studies using [^{18}F]FCWAY have shown some bone uptake of radioactivity due to defluorination and studies of the acid metabolite of [^{18}F]FCWAY indicated cranial uptake in the monkeys at later times (Carson et al., 2003). In the monkey [^{18}F]mefway studies that we have previously reported (Saigal et al., 2006; Wooten et al., 2011a, 2011b, 2012), cranial uptake was not evident. In light of the defluorination findings of [^{18}F]FCWAY, and more recent rodent studies of defluorination in bridgehead [^{18}F]fluorine derivatives based on the WAY-100635 skeleton (Hussainy et al., 2012) we examined the *in vivo* behavior of [^{18}F]FMCHA, the acid metabolite of [^{18}F]mefway (Fig-8). Accumulation of [^{18}F]FMCHA was primarily in the liver (Fig-8B) and uptake in the brain was negligible, and bone uptake did not increase with time. A more detailed analysis of the brain (Fig-8C) did not show any significant uptake over the course of the PET scan. Using the coregistered PET/CT scans of [^{18}F]mefway, certain areas of skull uptake were identified (Fig-3, asterisk shows skull uptake) which is likely a combination of [^{18}F]FMCHA and [^{18}F]fluoride ion.

In order to minimize breakdown of the amide linkage in [^{18}F]FCWAY and minimize defluorination, an innovative approach was used to inhibit the liver isozyme, cytochrome oxidase P450 (CYP2EI) using miconazole and minimize defluorination (Tipre et al., 2006). The use of miconazole increased the hippocampus to cerebellum ratio 3-fold. Similar experiments using miconazole and flucanozole (which is an inhibitor of the microsomal liver enzymes, CYP3A) have recently been reported in rats with [^{18}F]mefway which increased the uptake of [^{18}F]mefway in the brain while reducing cranial uptake (Choi et al., 2012). In our preliminary experiments with miconazole, measurement of BP_{ND} were not significantly affected by the presence or absence of miconazole. However, more detailed studies are planned in order to evaluate the role of CYP3A inhibitors in the rodent model for quantitation of smaller brain regions such as the dorsal raphe nucleus.

Binding potential (BP_{ND}) values for [^{18}F]mefway from PET studies across the different species (mice, rats and monkeys, Table-1) indicate that the hippocampus has the highest concentration of 5-HT_{1A} receptors. Additionally, the anterior cingulate cortex and the lateral

septal nuclei are both highly enriched with 5-HT_{1A} receptors The size of the brain corresponding to their body weights (mouse (25g), rat (250g) and monkey (10,000g)) affected the ability to quantitate smaller brain regions such as the dorsal raphe. Because of constraints of the resolution of the Inveon PET (Constantinescu and Mukherjee, 2009), measurements of BP_{ND} in the dorsal raphe in mice posed a challenge. Measurements in the rat were possible but underestimated relative to those measured in the monkeys. Although small differences in receptor distribution across the different species cannot be ruled out, our *in vitro* and *ex vivo* measures of [^{18}F]mefway binding suggested a high degree of binding of [^{18}F]mefway in the dorsal raphe of the mice and rats with high ratios versus the cerebellum. Comparing the in vivo rat PET in Table-1 and the *ex vivo* autoradiographic analysis in Table-2, there is approximately a 4 to 5-fold underestimation in the rat hippocampus for [^{18}F]mefway in the *in vivo* PET study. This discrepancy between *in vivo* findings and *ex vivo* analysis is consistent with our findings for other receptor systems (Bieszczcad et al., 2012), and is suggestive of recovery coefficient issues and partial volume issues that affect *in vivo* imaging.

Because [^{18}F]mefway may have some advantage over other PET imaging agents for 5-HT_{1A} receptors when applied to small animals, the use of interval ratio method would allow quantitative PET scans of rodents initiated at 60 min after radioligand injection and terminated at 70-90 min. In light of the radioactive half-life of [^{18}F]fluorine, this protocol could provide PET data of 5 rats or 10 mice with a single radiosynthesis of [^{18}F]mefway, which is not enabled by [^{11}C]WAY100635 due to its shorter half-life and [^{18}F]MPPF due to its faster kinetics. This will require a more thorough validation of the interval ratio method for [^{18}F]mefway studies in comparison with the Logan method using cerebellum as the reference region as well as by using plasma input function. Successful validation of interval ratio method will help increase the throughput of the rodent imaging experiments for various applications using a single radiopharmaceutical preparation.

5. CONCLUSION

The *trans*-isomer of mefway exhibits high affinity for the serotonin 5-HT_{1A} receptor sites. Our comparative imaging results from *in vivo* and *ex vivo* rat brains confirm that [^{18}F]mefway binds to the known 5-HT_{1A} receptor regions including the dorsal raphe. Our findings support that the dorsal raphe is measureable in rat PET studies. In mice receptor rich regions such as the hippocampus and frontal cortex were quantified, but quantification of dorsal raphe signal *in vivo* may be difficult. Our findings will be useful for staging rodent model studies using [^{18}F]*trans*-mefway because of its longer physical half-life (compared to [^{11}C]WAY-100635) and appropriate kinetics (compared to [^{18}F]MPPF) as an imaging agent for diagnosis, and potential therapy planning of 5-HT_{1A} receptor related disorders.

Acknowledgments

This research was financially supported by a grant from National Institutes of Health, R21/R33 AG 030524. We like to thank Drs. Min-Liang Pan, Evegueni Sevrioukov and M. Reza Mirbolooki and Dr. Bradley Christian for helpful discussion. We also like to thank Christopher Liang for technical assistance, Dustin Wooten for helpful discussions and the reviewers for their valuable suggestions. We thank Mr. Said Shokair at the Undergraduate Research Opportunities Program (UROP) of the University of California-Irvine for summer support (AKB) through the ID-SURE program.

REFERENCES

Akimova E, Lanzenberger R, Kasper S. The serotonin-1A receptor in anxiety disorders. Biol. Psychiatry. 2009; 66:627–635. [PubMed: 19423077]

Assem-Hilger E, Lanzenberger R, Savli M, Wadsak W, Mitterhauser M, Mien LK, Stogmann E, Baumgartner C, Kletter K, Asenbaum S. Central serotonin 1A receptor binding in temporal lobe epilepsy: A carbonyl-^{11}C-WAY-100635 PET study. Epilepsy Behav. 2010; 19:467–473. [PubMed: 20850389]

Bellido I, Diaz-Cabiale Z, Jimenez-Vasquez PA, Andbjer B, Mathe AA, Fuxe K. Increased density of galanin binding sites in the dorsal raphe in a genetic rat modelo f depression. Neurosci. Lett. 2002; 11:101–105. [PubMed: 11755250]

Bert B, Fink H, Rothe J, Walstab J, Bonisch H. Learning and memory in 5-HT$_{1A}$ receptor mutant mice. Behav Brain Res. 2008; 195:78–85. [PubMed: 18396339]

Bieszczcad K, Kant R, Constantinescu C, Pandey S, Kawai HD, Metherate R, Weinberger NM, Mukherjee J. Nicotinic acetylcholine receptors in the rat forebrain that bind [^{18}F]Nifene; relating PET imaging, autoradiography and behavior. Synapse. 2012; 66:418–434. [PubMed: 22213342]

Borg J. Molecular imaging of the 5-HT$_{1A}$ receptor in relation to human cognition. Behav Brain Res. 2008; 195:108–111.

Carson RE, Wu Y, Lang L, Ma Y, Der MG, Herscovitch P, Eckelman WC. Brain uptake of the acid metabolites of F-18-labeled WAY-100635 analogs. J Cereb Blood Flow Metab. 2003; 2:249–60. [PubMed: 12571456]

Cheng YC, Prusoff WH. Relationship between the inhibition constant and the concentration of inhibitor which cause 50 percent of an enzymatic reaction. Biochem Pharmacol. 1973; 22:3099–3108. [PubMed: 4202581]

Choi JY, Kim CH, Jeon TJ, Kim BS, Yi CH, Woo KS, Seo YB, Han SJ, Kim KM, Yi DI, Lee M, Kim DG, Kim JY, Lee KC, Choi TH, An G, Ryu YH. Effective microPET imaging of brain 5-HT$_{1A}$ receptors in rats with [^{18}F]mefway by suppression of radioligand defluorination. Synapse. 2012; 66:1015–1023. [PubMed: 22927318]

Coenen HH, Elsinga PH, Iwata R, Kilbourn MR, Pillai MRA, Rajan MGR, Wagner HN, Zaknun JJ. Fluorine-18 radiopharmaceuticals beyond [^{18}F]FDG for use in oncology and neurosciences. Nucl Med Biol. 2010; 37:727–740. [PubMed: 20870148]

Constantinescu CC, Mukherjee J. Performance evaluation of an Inveon PET preclinical scanner. Phys. Med. Biol. 2009; 54:2885–2899. [PubMed: 19384008]

Constantinescu CC, Sevrioukov E, Garcia A, Pan ML, Mukherjee J. Evaluation of [^{18}F]mefway biodistribution and dosimetry based on whole-body PET imaging of mice. Mol Imag Biol. 2012 [Epub ahead of print].

Costes N, Merlet I, Ostrowsky K, Faillenot I, Lavenne F, Zimmer L, Ryvlin P, LeBars D. A [^{18}F]MPPF PET normative database of 5-HT$_{1A}$ receptor binding in men and women over aging. J. Nucl. Med. 2005; 46:1980–1989. [PubMed: 16330560]

Dinh T, Faheem S, Rana N, Saigal N, Pandey S, Pan ML, Head E, Mukherjee J. Imaging serotonin receptors using [^{18}F]mefway in aging. J. Cereb. Blood Flow and Metabolism. 2009; 29:S357.

Duncan GE, Knapp DJ, Bresse GR, Crews FT, Little KY. Species differences in regional patterns of [^{3}H]8-OH-DPAT and [^{3}H]Zolpidem binding in the rat and human brain. Pharm Biochem Behav. 1998; 60:439–448.

Hussainy RA, Verbeek J, van der Born D, Molthoff C, Booij J, Herscheid JK. Synthesis, biodistribution and PET studies in rats of [^{18}F]Labeled bridgehead fluoromethyl analogues of WAY-100635. Nucl Med Biol. 2012; 39:1068–76. [PubMed: 22609028]

Ito H, Hietala J, Blomqvist G, Halldin C, Farde L. Comparison of the transient equilibrium and continuous infusion method for quantitative PET analysis of [^{11}C]raclopride binding. J Cereb Blood Flow Metab. 2011; 18:941–950. 2011. [PubMed: 9740097]

Khawaja X. Quantitative autoradiographic characterization of the binding of [^{3}H] WAY-100635, a selective 5-HT$_{1A}$ receptor antagonist. Brain Res. 1995; 673:217–225. [PubMed: 7606435]

Khawaja X, Evans N, Reilly Y, Ennis C, Minchin MCW. Characterization of the binding of [^{3}H] WAY-100635, a Novel 5-Hydroxytryptamine1A Receptor Antagonist, to Rat Brain. J Neurochem. 1995; 6:2718–2719.

King MV, Marsden CA, Fone KC. A role for the 5-HT$_{1A}$, 5-HT$_{4}$ and 5-HT$_{6}$ receptors in learning and memory. Trends Pharmacol. Sci. 2008; 29:482–492. [PubMed: 19086256]

Kennedy SE, Zubieta JK. Neuroreceptor imaging of stress and mood disorders. CNS Spectrums. 2004; 9:292–301. [PubMed: 15048054]

Kepe V, Barrio JR, Huang SC, Ercoli L, Siddarth P, Shoghi-Jadid K, Cole GM, Satyamurthy N, Cummings JL, Small GW, Phelps ME. Serotonin 1A receptors in the living brain of Alzheimer's disease patients. Proc Natl Acad Sci U S A. 2006; 3:702–707. [PubMed: 16407119]

Lammertsma AA, Hume SP. Simplified reference tissue model for PET receptor studies. Neuroimage. 1996; 4:153–158. [PubMed: 9345505]

Lanzenberger R, Baldinger P, Hahn A, Ungersboeck J, Mitterhauser M, Winkler D, Micskei Z, Stein P, Karanikas G, Wadsak W, Kasper S, Frey R. Global decrease of serotonin-1A receptor binding after electroconvulsive therapy in major depression measured by PET. Mol. Psychiatry. 2013; 18:93–100. [PubMed: 22751491]

Logan J, Fowler JS, Volkow ND, Wang GJ, Ding YS, Alexoff DL. Distribution volume ratios without blood sampling from graphical analysis of PET data. Journal of Cerebral Blood Flow and Metabolism. 1996; 16:834–840. [PubMed: 8784228]

Ma Y, Hof PR, Grant SC, Blackband SJ, Bennett R, Slatest L, McGuigan MD, Benveniste H. A three-dimensional digital atlas database of the adult C57BL/6J mouse brain by magnetic resonance microscopy. Neuroscience. 2005; 135:1203–1215. [PubMed: 16165303]

Mehrotra S, Gupta S, Chan KY, Villalon CM, Centurion D, Saxena PR, MassenVanDenBrink A. Current and prospective pharmacological targets in relation to antimigraine action. Naunyn-Schmiedeberg's Arch Pharmacol. 2008; 378:373–374.

Parsey RV. Serotonin receptor imaging: Clinically useful? J. Nucl. Med. 2010; 51:1495–1496. [PubMed: 20847181]

Parsey RV, Slifstein M, Hwang DR, Abi-Dargham A, Simpson N, Mawlawi O, Guo NN, Van Heertum R, Mann JJ, Laruelle M. Validation and reproducibility of measurement of 5-HT_{1A} receptor parameters with [carbonyl-^{11}C]WAY-100635 in humans: comparison of arterial and reference tissue input functions. J Cereb Blood Flow Metab. 2000; 7:1111–33. [PubMed: 10908045]

Paterson LM, Kornum BR, Nutt DJ, Pike VW, Knudsen GM. 5-HT radioligands for molecular brain imaging with SPECT and PET. Med. Res. Rev. 2013; 33:54–111. [PubMed: 21674551]

Paxinos, G.; Watson, C. The Rat Brain in Stereotaxic Coordinates. Academic Press; Sidney: 1986.

Pike VW. PET Radiotracers: crossing the blood-brain barrier and surviving metabolism. TiPs. 2009; 30:431–440. [PubMed: 19616318]

Saigal N, Pichika R, Balasubramaniam E, Collins D, Christian BT, Shi B, Narayanan TK, Potkin SG, Mukherjee J. Synthesis and biologic evaluation of a novel serotonin 5-HT_{1A} receptor radioligand, [^{18}F]Labeled mefway, in rodents and imaging by PET in a nonhuman primate. J Nuc Med. 2006; 47:1697–1706.

Saijo T, Maeda J, Okauchi T, Maeda J-I, Morio Y, Kuwahara Y, Suzuki M, Goto N, Fukumura T, Suhara T, Higuchi M. Presynaptic selectivity of a ligand for serotonin 1A receptors revealed by *in vivo* PET assays of rat brain. PLoS ONE. 2012; 7(8):e42589. [PubMed: 22880045]

Savitz J, Lucki I, Dreverts WC. 5-HT_{1A} receptor function in major depressive disorder. Prog. Neurobiol. 2009; 88:17–31. [PubMed: 19428959]

Schweinhardt P, Fransson P, Olson L, Spenger C, Andersson JL. A template for spatial normalisation of MR images of the rat brain. J Neurosci Methods. 2003; 129:105–113. [PubMed: 14511814]

Tipre DN, Zoghbi SS, Liow JS, Green MV, Seidel J, Ichise M, Innis RB, Pike VW. PET imaging of brain 5-HT_{1A} receptors in rat *in vivo* with [^{18}F]FCWAY and improvement by successful inhibition of radioligand defluorination with miconazole. J Nucl Med. 2006; 47:345–53. [PubMed: 16455642]

Truchot L, Costes SN, Zimmer L, Laurent B, Le Bars D, Thomas-Anterion C, Mercier B, Hermier M, Vighetto A, Krolak-Salmon P. A distinct [^{18}F]MPPF PET profile in amnestic mild cognitive impairment compared to mild Alzheimer's disease. Neuroimage. 2008; 40:1251–1256. [PubMed: 18313943]

Wooten DW, Hillmer AT, Moirano JM, Ahlers EO, Slesarev M, Barnhart TE, Mukherjee J, Schneider ML, Christian BT. Measurement of 5-HT_{1A} receptor density and *in vivo* binding parameters of

[^{18}F]mefway in the nonhuman primate. J Cereb Blood Flow Metab. 2012; 32:1546–1558. [PubMed: 22472611]

Wooten D, Hillmer A, Murali D, Barnhart T, Schneider ML, Mukherjee J, Christian BT. An *in vivo* comparison of *cis*- and *trans*-[^{18}F]mefway in the nonhuman primate. Nucl Med Biol. 2011a; 38:925–32. [PubMed: 21741252]

Wooten DW, Moraino JD, Hillmer AT, Engle JW, Dejesus OJ, Murali D, Barnhart TE, Nickles RJ, Davidson RJ, Schneider ML, Mukherjee J, Christian BT. *In vivo* kinetics of [F-18]mefway: a comparison with [C-11]WAY100635 and [F-18]MPPF in the nonhuman primate. Synapse. 2011b; 65:592–600. [PubMed: 21484878]

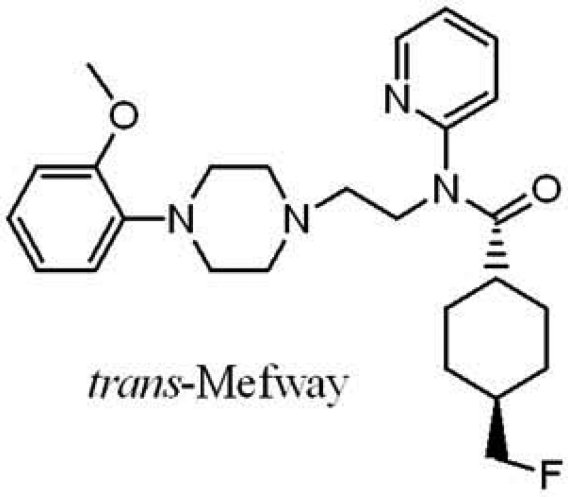

trans-Mefway

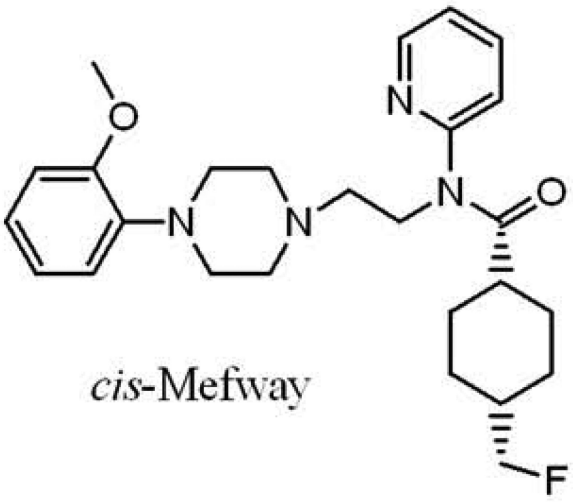

cis-Mefway

Figure 1.
Chemical structure of [^{18}F]*trans*-mefway and [^{18}F]*cis*-mefway.

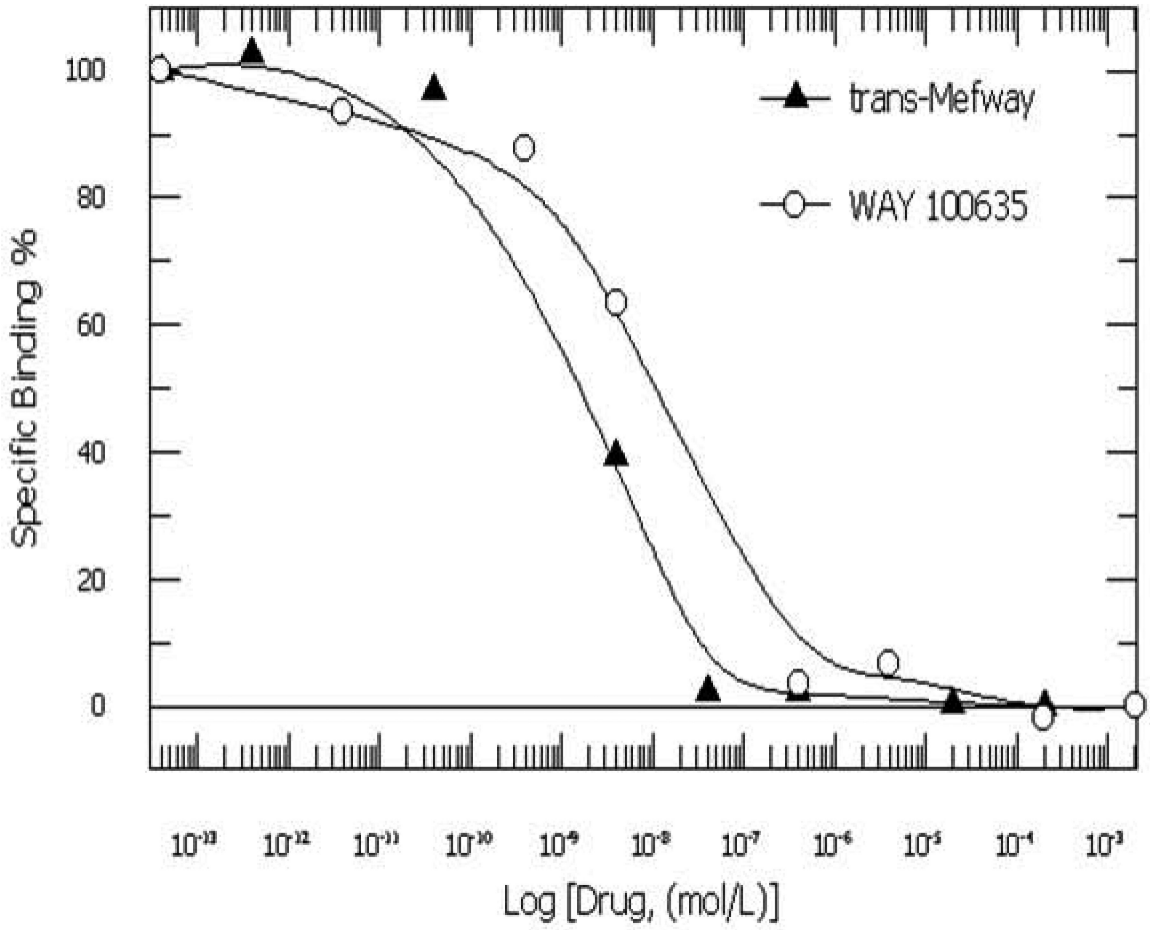

Figure 2.
Displacement curves of mefway and WAY-100635 measured in rat brain homogenates using [^{3}H]WAY-100635 for the serotonin 5-HT$_{1A}$ receptor sites.

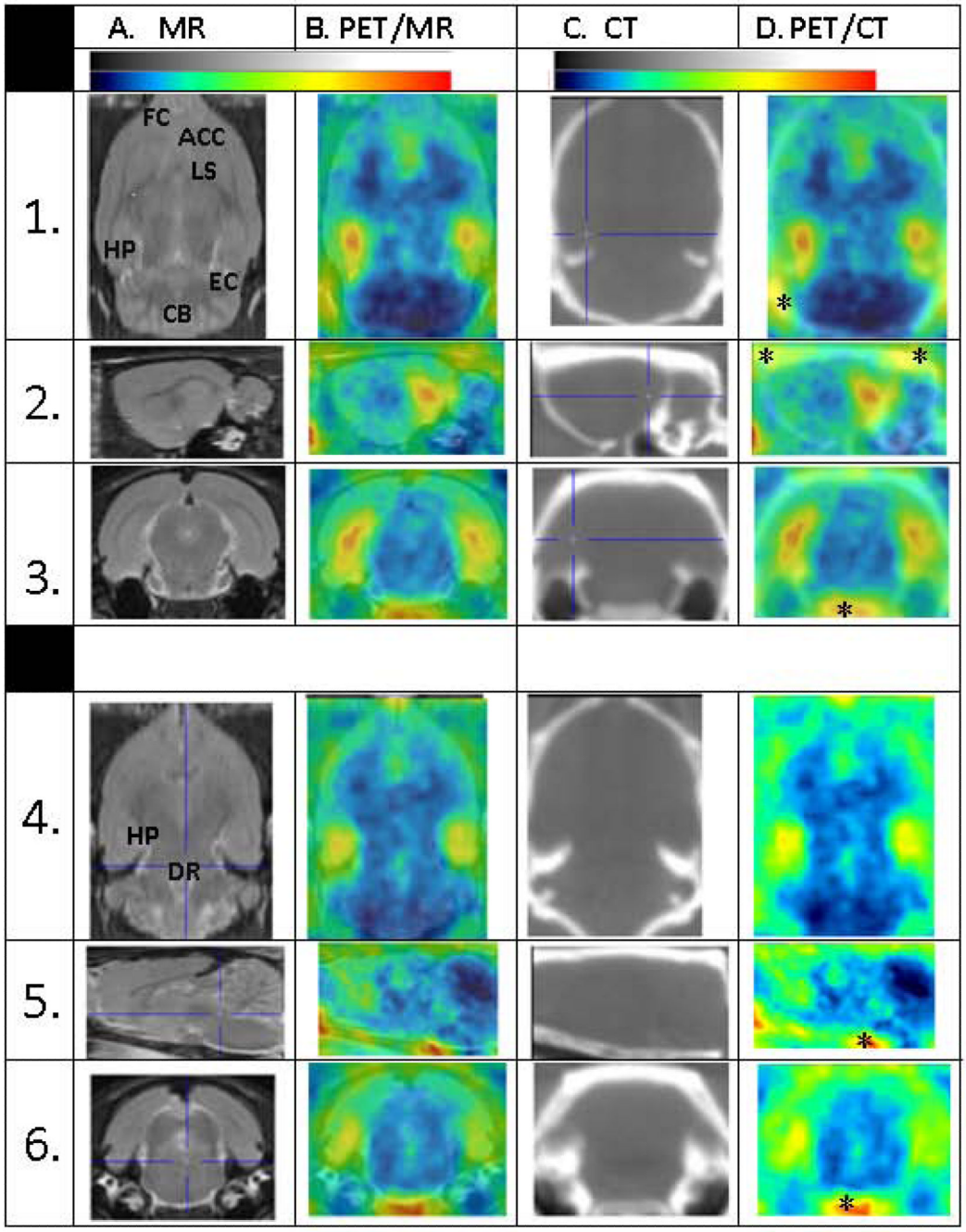

Figure 3.

PET/CT imaging of rats showing two different orthogonal planes. PET images were summed from 60 to 90 min, postinjection: (**A**). MR template images of the rat brain; (**B**). [^{18}F]Mefway PET/MR images at two different planes; through the dorsal hippocampus and through the ventral hippocampus and dorsal raphe. (**C**). CT images showing brain and skull; (**D**). Coregistered CT images of mefway PET. Asterisks indicate radioactivity containing areas outside the brain confirmed by coregistered CT.

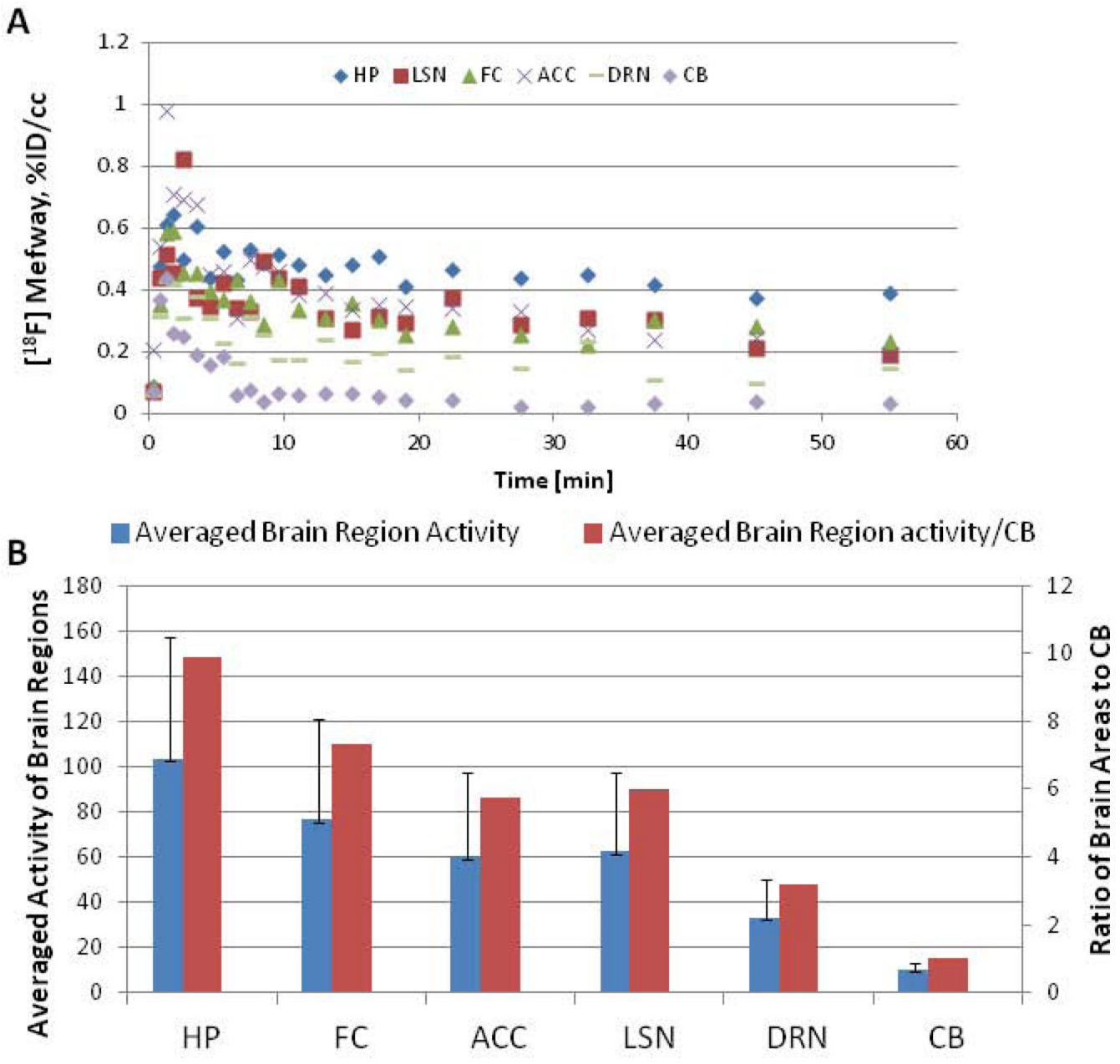

Figure 4.

(**A**). Time-activity curve of [^{18}F]mefway in the rat brain showing hippocampus (HP), lateral septum (LSN), frontal cortex (FC), anterior cingulate cortex (ACC), dorsal raphe nucleus (DRN) and cerebellum (CB). (**B**). Averaged *in vivo* brain activity of rats (n=4) in the different brain regions measured by PET and brain region to cerebellum ratios.

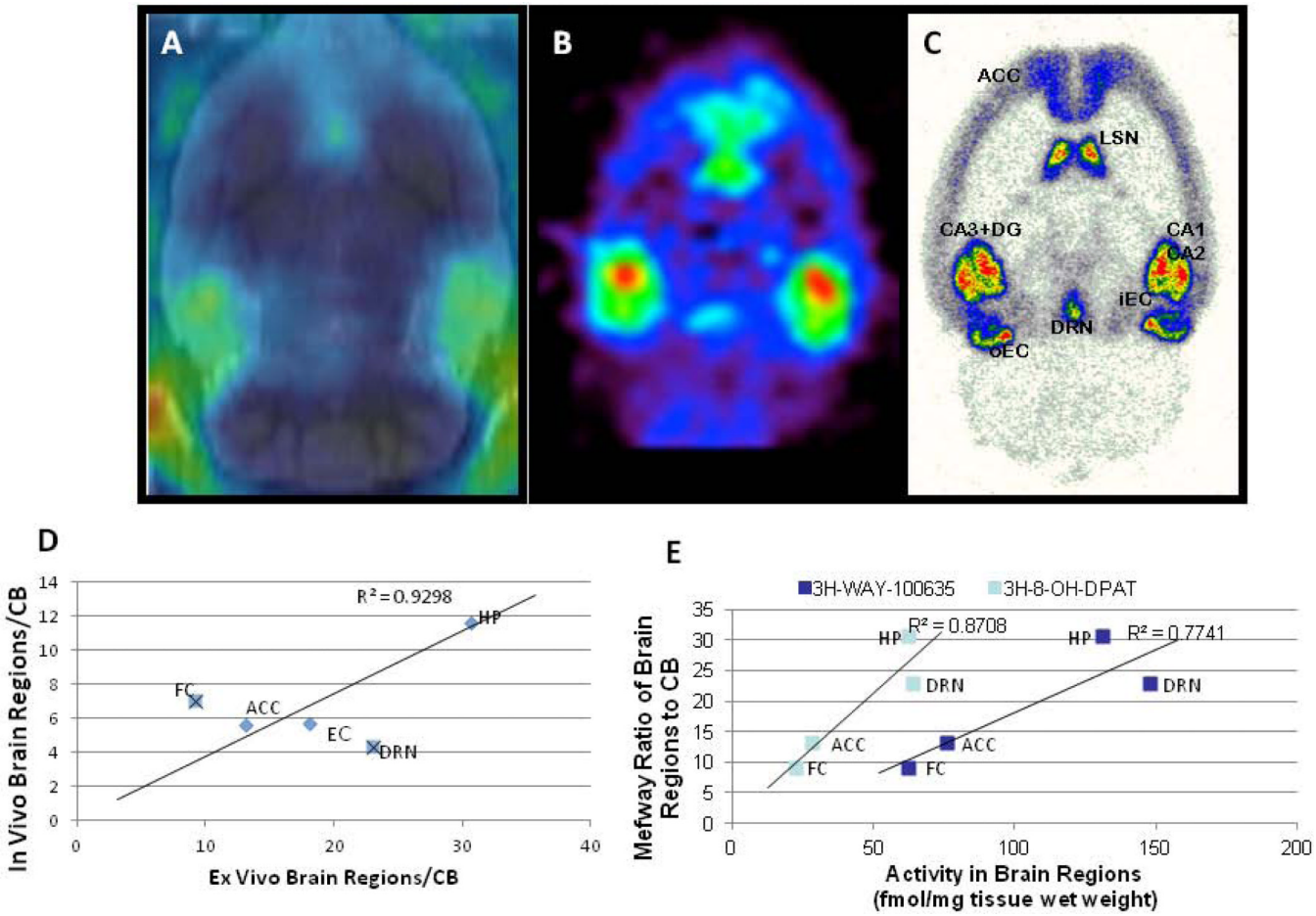

Figure 5.

(**A**). *In vivo* PET rat brain slice of [^{18}F]mefway coregistered to MR template after injection of 24.6 ± 11.3 MBq dose of [^{18}F]mefway. (**B**). *Ex vivo* PET of [^{18}F]mefway taken immediately after completion of the *in vivo* PET scan. (**C**). After the *ex vivo* scan is completed, the brain is cut into 40micron sections and exposed to phosphor screens. (**D**). Correlation of [^{18}F]mefway binding in vivo (A) with the *ex vivo* autoradiographs (C). Correlation is high when the frontal cortex and dorsal raphe nucleus are excluded. (**E**). Correlation of [^{18}F]mefway binding ratio with reported binding of [^{3}H]8-OH-DPAT in different brain regions.

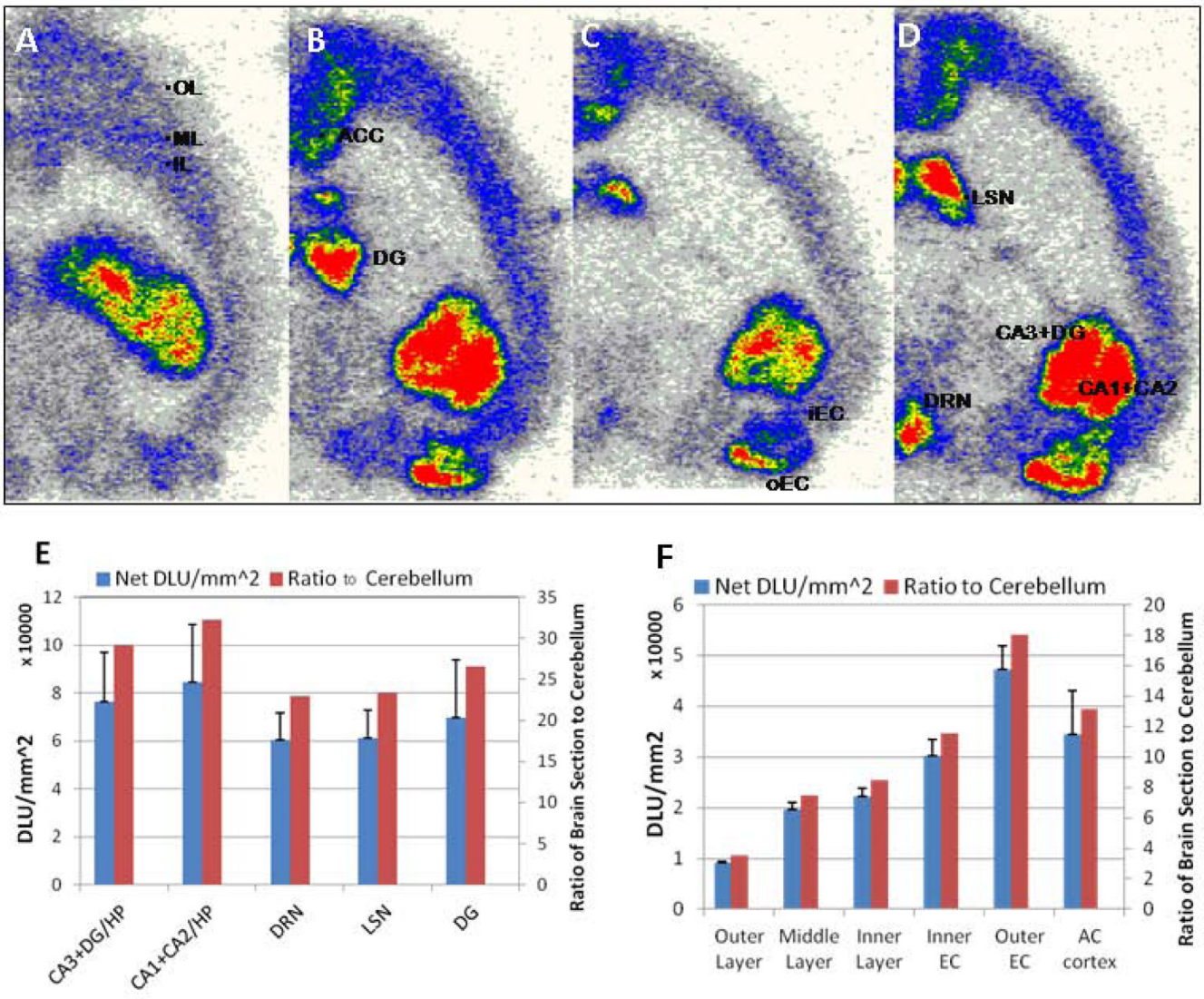

Figure 6.

(**A-D**). *Ex vivo* horizontal brain slices of rodent brain showing binding of [^{18}F]mefway (red = highest binding and white = lowest binding; OL=outer layer of cortex; ML= middle layer of cortex; IL=inner layer of cortex; ACC=anterior cingulated cortex; DG= dentate gyrus; iEC= inner enthorinal cortex; oEC= outer enthorinal cortex; LS= lateral septal nuclei; DRN= dorsal raphe nucleus; CA1, CA2, CA3= hippocampal regions). (**E**). Quantitation of [^{18}F]mefway binding in hippocampal regions, dorsal raphe and septal nuclei in *ex vivo* autradiographs and ratio with respect to the cerebellum; (**F**). Quantitation of [^{18}F]mefway binding in cortical layers in *ex vivo* autradiographs and ratio with respect to cerebellum.

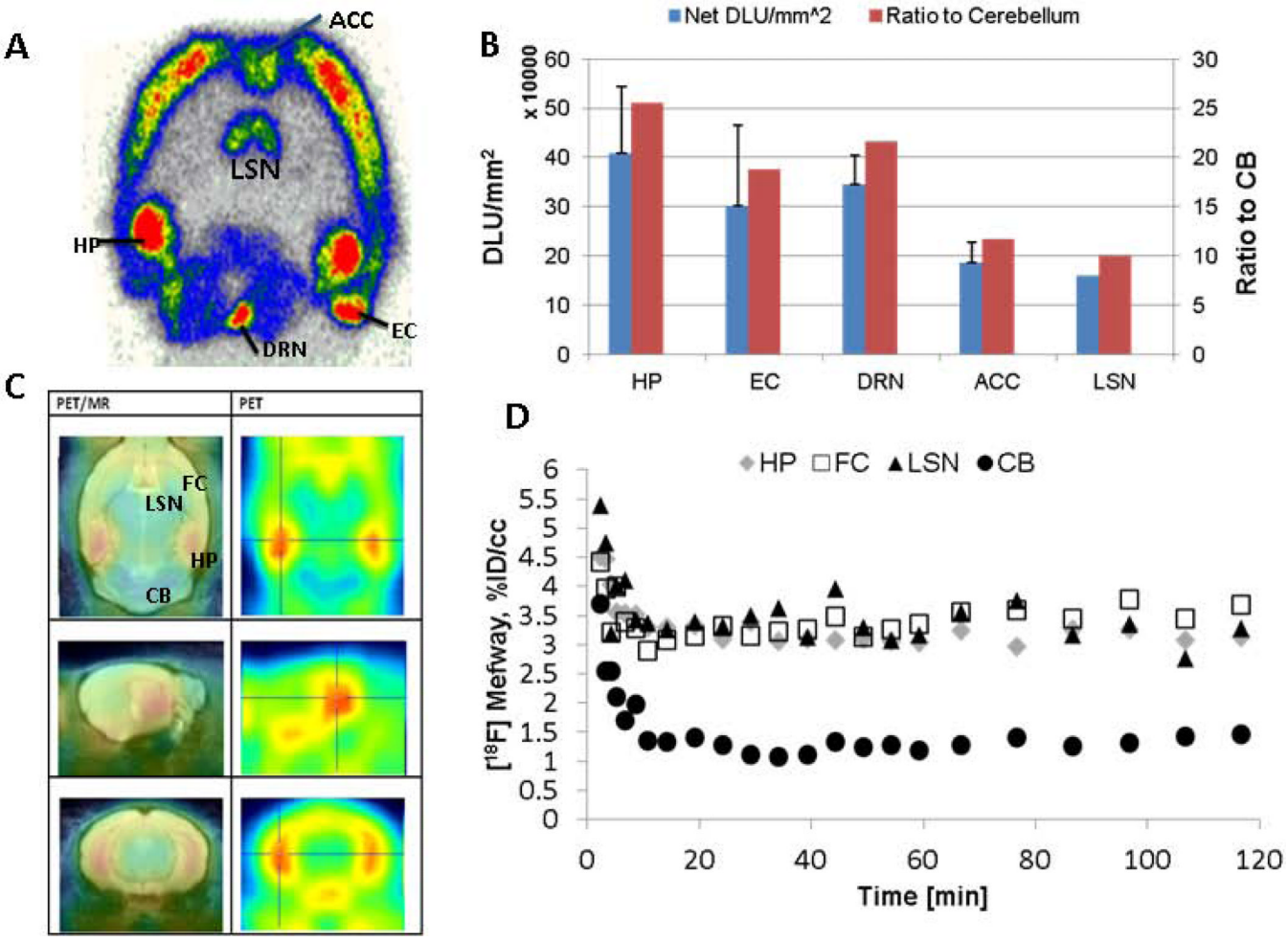

Figure 7.

[^{18}F]Mefway PET imaging of mice: (**A**). Horizontal mouse brain section showing [^{18}F]mefway binding, ACC= anterior cinglate cortex; LS= lateral septal nuclei; HP= hippocampus; DRN= dorsal raphe nucleus; EC= enthorinal cortex); (**B**). Time-activity curves of [^{18}F]mefway in the mouse brain; (**C**). PET images were summed from 60 to 90 min, postinjection and coregistered with mouse brain MR template to show [^{18}F]Mefway PET/MR images of mice through the dorsal hippocampus. (**D**). Quantitation of [^{18}F]mefway in the mouse brain regions and ratios with respect to cerebellum.

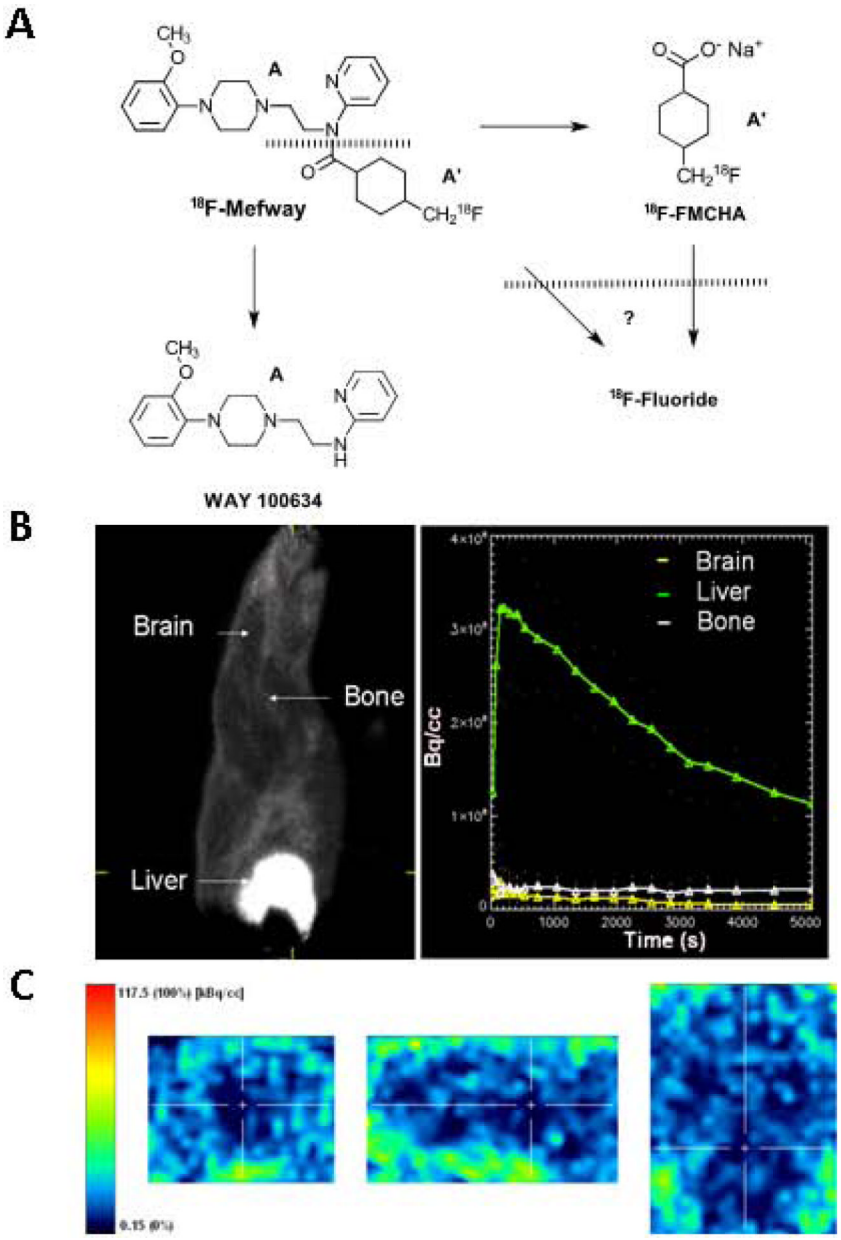

Figure 8.

(**A**). Schematic showing potential breakdown of [^{18}F]mefway at the amide linkage to provide the [^{18}F]*trans*-4-fluoromethylcyclohxane carboxylate ([^{18}F]FMCHA) and WAY-100634. Decompostion of [^{18}F]FMCHA and [^{18}F]mefway may further occur to give [^{18}F]fluoride ion. (**B**). Rat summed of [^{18}F]FMCHA showing upper body including head and liver of [^{18}F]FMCHA distribution and time activity curves of various regions of the body; (**C**). Brain slices showing little [^{18}F]FMCHA.

TABLE 1

PET MEASURES OF BRAIN UPTAKE OF ^{18}F-MEFWAY IN VARIOUS SPECIES

Brain Regions	Mouse In Vivo PET[a]	Rat In Vivo PET[b]	Monkey In vivo PET[c]
Hippocampus (or MTC)	1.15	6.41	7.36
ACG (or ACC)	-	3.71	7.15
Dorsal Raphe	-	1.23	3.69
Insular cortex	-	-	4.16
LSN	0.99	4.05	-
Frontal cortex	1.27	5.48	-

[a] Average BP_{ND}(n=3) measured using interval ratio method (Ito et al., 2011).

[b] Average BP_{ND}(n=4) measured from Logan analysis, 1996.

[c] BP_{ND} values in rhesus monkeys (taken from Wooten et al., 2001b).

TABLE 2

AUTORADIOGRAPHIC ANALYSIS OF ^{18}F-MEFWAY IN VARIOUS SPECIES

Brain Regions	Mouse In vitro[a]	Rat In vitro[b]	Rat Ex vivo[c]
HP	25.6	51.4	30.7
LSN	10.0	38.1	23.4
EC	18.8	34.9	14.8
DRN	21.7	41.2	23.0
DG	--	41.6	26.6
ACC	11.6	28.2	13.1
CB	1	1	1

[a] Average ratios measured from in vitro brain sections shown in Fig-7B.

[b] Average ratios measured from rat brain in vitro binding.

[c] Average ratios measured from in vitro brain sections shown in Fig-6.